Novel Electronic Structure of a Highly Strained Oxide Interface

The misfit oxide, $Bi_2Ba_{1.3}K_{0.6}Co_{2.1}O_{7.94}$, made of alternating rocksalt-structured [BiO/BaO] layers and hexagonal CoO_2 layers, was studied by angle-resolved photoemission spectroscopy. The detailed electronic structure of a highly strained oxide interface is revealed for the first time. The large strain in the rocksalt layer induces a large electron transfer to the less strained CoO_2 layer. At the presence of two incommensurate crystal fields, the low-energy electronic states of each individual layer are confined within itself; but they undergo umklapp scattering by the incommensurate crystal field from the neighbouring layer. Furthermore, a novel interfacial enhancement of electron-phonon interactions (likely with interfacial phonons) is discovered. These novel electronic properties depict a detailed microscopic picture of various important processes that could occur at oxide interfaces in general.

Beamline
21B1 U9 – (CGM)

Authors
B. P. Xie, H. W. Ou, and D. L. Feng
Fudan Univesity, Shanghai, China

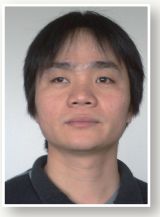

Oxide interfaces have attracted much attention for the emergence of novel phenomena, including high conductivity, even superconductivity and gigantic thermoelectric effect. A thorough understanding of the microscopic processes at the oxide interface is the first step toward designing functional heterostructures. Angle-resolved photoemission spectroscopy (ARPES) is a powerful technique for studying electronic structure of novel materials. [1-4] Pioneering angle-integrated photoemission experiments have been conducted on pulsed-laser deposited oxide interfaces. However, because of the short mean free path of photoelectrons, photoemission signals from the interface are very weak, which forbids high resolution and momentum resolved measurements. The recent synthesized misfit oxide single crystals provide an alternative solution. Since each unit cell of a misfit oxide is usually composed of two kinds of oxide layers with distinct symmetries, it resembles a very clean artificial heterostructure and is suitable for photoemission experiments. Among them, misfit structured oxide, $Bi_2Ba_{1.3}K_{0.6}Co_{2.1}O_{7.94}$ (BBKCO) possesses the highest thermoelectric power and high conductivity in its class, and thus high figure of merit for thermoelectric applications. Its structure, as shown in Fig. 1(a), consists of rocksalt-structured [BiO/BaO] layers and hexagonal CoO_2 layers with edge-shared CoO_6 octahedra, and K^+ and Co^{3+} ions are doped into the BaO layer. The two adjacent BiO layers are weakly bound by the van der Waals force, providing a stable BiO natural cleavage plane. This is shown by the rectangular low-energy electron diffraction pattern in Fig. 1(b). The [BiO/BaO] layers are orthorhombic, the lattice constants along the two Bi-O-Bi bond directions are a_{RS} = 5.031 Å, b_{RS} = 5.683 Å, respectively. a_{RS} matches the distance between the neighbouring Co ions along the same direction, while for the perpendicular direction, b_{RS} = 1.97 b_{CoO2} , which is collinear but aperiodic, causes the global misfit of the lattice. The CoO_2 sublattice preserves the structure of its freestanding form, close to that in Na_xCoO_2. However, the [BiO/BaO] sublattice is largely distorted compared with the BiO, BaO layers in cuprate superconductors $Bi_2Sr_2CaCu_8O_{8+y}$ and $YBa_2Cu_3O_{7-x}$. It is

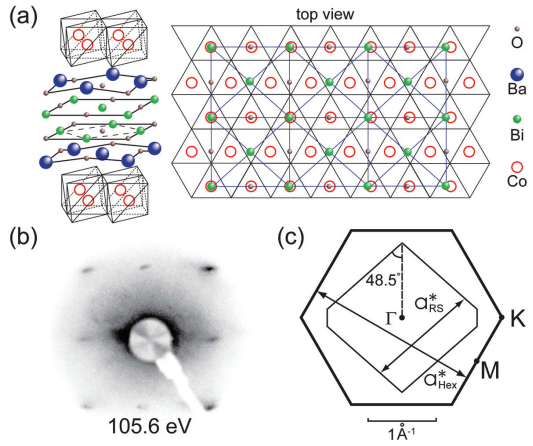

Fig. 1: (a) A schematic picture of the crystal structure of $Bi_2M_2Co_2O_y$ (M= Ca, Sr, Ba). The oxygen atoms in the CoO_2 layers and BaO layer in the topview are omitted for simplicity. (b) Low-energy electron diffraction pattern exhibits the four-fold symmetry of the orthorhombic BiO surface of $Bi_2Ba_{1.3}K_{0.6}Co_{2.1}O_{7.94}$. (c) The reduced Brillouin zones (BZ) for the rocksalt [BiO/BaO] layers (thin lines) and the hexagonal CoO_2 layer (thick lines). The corresponding reciprocal lattice constants a_{RS}* and a_{Hex}* are also illustrated.

squeezed by 6.4% along the a_{RS} direction, while elongated by about 5.75% along the b_{RS} direction. Furthermore, the Ba^{2+} ions are displaced from the BaO plane towards the oxygen ions of the CoO_2 layer by 0.4 Å. These huge displacements and the misfit indicate large strain in the rocksalt layer. The reduced Brillouin zones for the individual [BiO/BaO] layers and CoO_2 layer are plotted in Fig. 1(c).

Two kinds of states with distinct photon energy dependence are identified for BBKCO. Figures 2(a)–2(f) show the photoemission intensity along the Γ-K direction taken with six different photon energies between 15 and 24 eV. With relatively low-energy photons [Figs. 2(a)–2(c)], photoemission data show only one feature that disperses towards K at higher binding energies. Correspondingly, the map of photoelectron intensity at the Fermi energy (E_F) gives a hexagonal holetype Fermi pocket centred around Γ in Fig. 2(g) (dashed lines). This resembles the Fermi surface (FS) observed in Na_xCoO_2, where the sixfold symmetry is clearly observed. With higher energy photons, another feature that disperses to the opposite direction becomes dominant [Figs. 2(d)–2(f)]. Correspondingly, in Fig. 2(h), four holetype Fermi pockets show up in the intensity map measured at 21.2 eV, which could be fitted with the four dash-dotted ellipses. These FS's with the symmetry of the rocksalt layer were not observed in previous ARPES works of other misfit Cobaltites. Clearly, they should be mostly originated from the [BiO/BaO] layers. The different origins of these bands enable us to unveil various interfacial effects, and explain the observed large photon energy dependence. Since the environment of [BiO/BaO] layer is asymmetric, while CoO_2 layer is symmetric along the c-axis, the distributions of their wave functions along the c-axis are very different. Upon varying photon energy, out-of-plane momentum (k_z) of the final state photoelectron varies. Consequently, the photoemission matrix elements are affected differently for states in different layers.

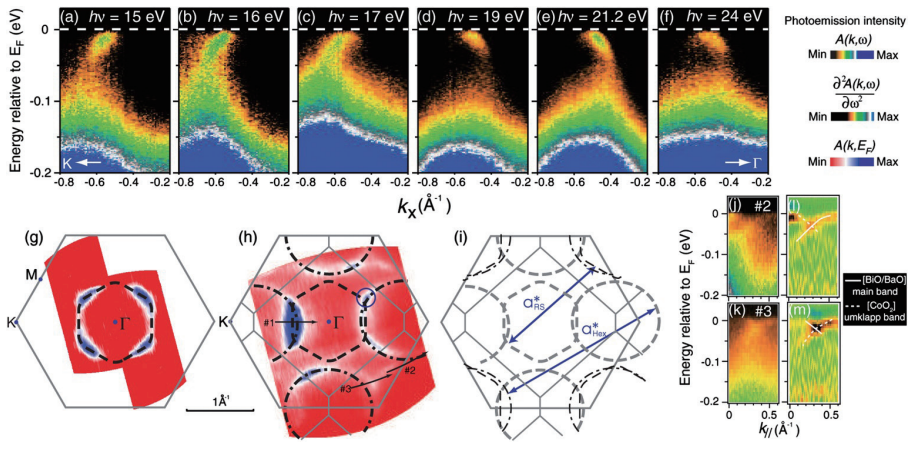

Fig. 2: ARPES data for $Bi_2Ba_{1.3}K_{0.6}Co_{2.1}O_{7.94}$ along the cut 1 direction with different photon energies: (a) 15 eV, (b) 16 eV, (c) 17 eV, (d) 19 eV, (e) 21.2 eV, (f) 24 eV photon energy. (g-h) Fermi Surfaces measured at 20 K with15 eV and 21.2 eV photons respectively, obtained by integration of the spectral weight in a 20 meV window around E_F. The dash-dotted and dashed thick curves are $[CoO_2]$-derived and [BiO/BaO]-derived Fermi pockets respectively. Their umklapp Fermi surfaces are indicated by thinner curves in (i), (j), (k). The photoemission intensity along cut 2 and 3 in panel h, respectively, and (l), (m) their second derivative with respect to energy to highlight the dispersion.

The van der Waals bond between two neighbouring BiO layers and the large resistivity

anisotropy in BBKCO suggest weak inter-unit-cell coupling. Consistently, the Fermi crossing momenta (k_F's) in Figs. 2(a)–2(f) show negligible dependency on the photon energies, which correspond to different k_z's. For a two dimensional state, one can estimate its occupancy through the FS volume based on the Luttinger theorem. The CoO_2 layers are usually stoichiometric, which would be half filled in undoped case. The measured FS volume indicates that each CoO_2 formula unit has 0.6 extra electrons from the [BiO/BaO] layers. The [BiO/SrO] layers in cuprate superconductors are prototypical charge reservoir, which donate holes to the CuO_2 plane. Normally, one would expect [BiO/BaO] layers to donate holes, especially when its Ba^{2+} ions are replaced with K^+ ions. However, the FS volume of the [BiO/BaO] rocksalt layers indicates that 0.6 electrons are missing for each [BiO/$Ba_{0.65}K_{0.3}Co_{0.05}O$] formula unit, which exactly matches the additional electrons in the CoO_2 layer. This large electron loss out of the [BiO/BaO] layers clearly demonstrates that huge strain would significantly raise the energy of electronic states. Consequently, the electrons flow into the low-energy states of the nearby layer. For BBKCO, this charge transfer would save the total energy significantly, and thus help stabilize the misfit structure. Furthermore, the exact electron and hole concentration match indicates that the systems are very close to its stoichiometric condition. Considering that a large Madelung potential would be induced by such a large charge transfer, there must be another channel for a "back-flow" of electrons; for example, by forming covalent bonds across the interface in the high lying states. Indeed, the evidence for such covalent bondings is found in the k_z dependence of the valence band dispersion along the Γ-K direction.

Strong interlayer couplings were observed for quantum well states at metal-semiconductor interfaces. Remarkably, the low-energy bands in different layers of BBKCO do not show any sign of hybridization, even though there is a large charge transfer in between. For example, in Fig. 2(h), the CoO_2 FS crosses the rocksalt layer FS without any sign of anticrossing. In particular, there is even a slight enhancement of spectral weight at the crossing momentum, as highlighted by the small blue circle. The observed two independent FS sets with distinct symmetries prove that the low-energy electronic states of [BiO/BaO] or CoO_2 layer are spatially confined within itself. This interesting finding is further evidenced by the detailed properties of the quasiparticles. Figures 3(a) and 3(b) show the photoemission images of the quasiparticles in the CoO_2 layer, and the [BiO/BaO] layers, respectively, along the Γ-K direction. As shown in Fig. 3(d), the measured quasiparticle scattering rate is a linear function of the binding energy for CoO_2 state, while it is a quadratic function near E_F for [BiO/BaO] state.

There are several weak FS features besides the main ones in Fig. 2(h). If one would displace the main FS of [BiO/BaO] layers by the reciprocal lattice constant a_{Hex}* of the CoO_2 layer [illustrated by the double-headed arrows in Fig. 2(i)], the resulting umklapp FS's (thin lines) perfectly fit these weak features in Fig. 2(h). Similarly, the CoO_2 umklapp FS's are observed apart from the main ones by the reciprocal lattice constant a_{RS}* of the [BiO/BaO] layers. Therefore, this proves that the crystal field from one side of the interface is imposed on the other, and acts as an incommensurate potential that scatters the electrons there. We note that the main [BiO/BaO] band and the umklapp CoO_2 band just cross each other without any sign of hybridization [Figs. 2(j)–2(m)], manifesting the weak coupling between the low-energy electronic states.

More interfacial effects are revealed by comparing the BBKCO data with those of $Na_{0.7}CoO_2$ taken in the same momentum region. While the $Na_{0.7}CoO_2$ dispersion is a smooth curve [Fig. 3(c)], there are strong kinks on the dispersions of the BBKCO bands [Figs. 3(a) and 3(b)]. These kinks are very robust as they show up independent of photon energy, suggesting an intrinsic effect due to

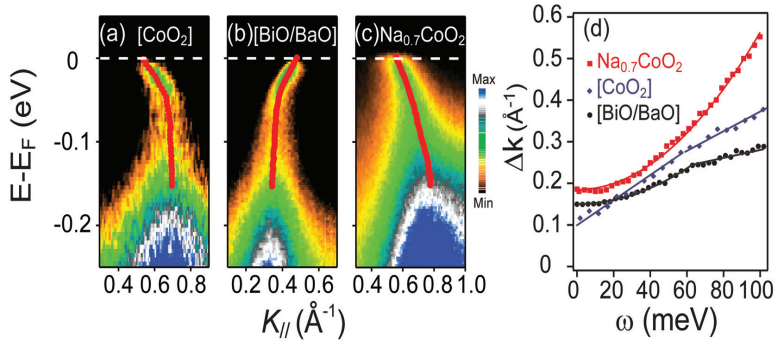

Fig. 3: Photoemission intensity along Γ – K taken at 20K, for (a) BBKCO's CoO_2 layer ($h\nu$=15eV), (b) BBKCO's [BiO/BaO] layers ($h\nu$=21.2eV), and (c) $Na_{0.7}CoO_2$ ($h\nu$=21.2eV). The thick curves are fitted dispersions. (d) The width of the momentum distribution curve vs. binding energy for data presented in panel a-c, which is an estimate of the quasiparticle scattering rate.

interactions with some bosonic modes. Since the doping for CoO_2 layers in BBKCO and $Na_{0.7}CoO_2$ are similar, the magnetic excitations should have similar strength in both cases. Therefore, the strong kinks here are most likely caused by phonons induced by the highly strained interface. Considering the nonmagnetic nature of the rocksalt layer, and similar kink energy scales, the kink of the rocksalt layer might be caused by the interface phonons as well. This strong coupling is also reflected in the quasiparticle scattering rate [Fig. 3(d)], where a clear turning point around 60 meV appears for both the bands of BBKCO. Furthermore, the scattering rate of $Na_{0.7}CoO_2$ is a simple quadratic function of binding energy, different from the linear behavior of the BBKCO CoO_2 layer. This suggests that the electronphonon interactions induced by the interface may change the quasiparticle behaviour.

To summarize, we have revealed various interfacial electronic properties that have never been observed in oxide interfaces before. The relation between strain and charge transfer across oxide interface is illustrated from a microscopic level. While the interactions between low energy states on two sides of the interface are weak, interlayer covalent bonding exists between high lying states. The enhancement of electron-phonon coupling and interfacial umklapp scattering are discovered. Our findings provide an electronic structure foundation for understanding oxide interfaces and some important guidelines for designing oxide devices.

Experimental Station

Angle-Resolved UPS end station

Publications

1. B. P. Xie, K. Yang, D. W. Shen, and J. F. Zhao, *et. al.*, Phys. Rev. Lett. **98**, 147001 (2007).
2. H. W. Ou, J. F. Zhao, Y. Zhang, and B. P. Xie, *et. al.*, Phys. Rev. Lett. **102**, 026806 (2009).
3. D. W. Shen, B. P. Xie, J. F. Zhao, and L. X. Yang, *et. al.*, Phys. Rev. Lett. **102**, 026806 (2009).
4. J. Wei, Y. Zhang, H. W. Ou, and B. P. Xie, *et. al.*, Phys. Rev. Lett. **101**, 097005 (2008).

Contacted E-mail

bpxie@fudan.edu.cn